



# Moiré physics in twisted van der Waals heterostructures of 2D materials

Sanjay K. Behura<sup>1,2</sup> · Alexis Miranda<sup>3</sup> · Sasmita Nayak<sup>1</sup> · Kayleigh Johnson<sup>1</sup> · Priyanka Das<sup>4</sup> · Nihar R. Pradhan<sup>4</sup>

Received: 1 February 2021 / Accepted: 18 June 2021  
© Qatar University and Springer Nature Switzerland AG 2021

## Abstract

Artificial moiré superlattices are formed by vertically stacking two monolayers of two-dimensional (2D) materials and rotating one of the layers with a finite twist angle. The resultant moiré pattern in the twisted heterostructures exhibits periodic length scale larger than that of lattice atoms of the individual layers. Furthermore, the moiré pattern is found to control the interlayer hybridization in a twisted bilayer heterostructure creating strongly correlated quantum states. Owing to the moiré pattern—introduced interlayer hybridization, several exotic quantum phenomena such as flat bands, moiré excitons, surface plasmon polaritons, surface phonon polaritons, surface exciton polaritons, interlayer magnetism, and 2D ferroelectricity are recently found in the engineered materials with additional twist degree of freedom. Here we review some notable advances in moiré physics associated with twisted bilayer heterostructures of 2D crystals including (A) flat bands in the twisted bilayer graphene, (B) exciton superlattices in the twisted transition metal dichalcogenides, (C) topological polaritons and photonic superlattices in the twisted 2D metal oxides, (D) interlayer magnetism in the stacked 2D magnetic semiconductors, and (E) ferroelectricity in moiré quantum materials. This story-of-twist begins with (1) an introduction to twisted heterostructures, (2) a correlation between van der Waals heterostructures and moiré superlattices, (3) how to design and fabricate moiré quantum materials, (4) discussion on five emergent quantum phenomena associated with twisted bilayer heterostructures as listed above, and finally (5) what are the challenges in fabrication, characterization, and applications of twisted heterostructures. This review concludes with an outlook pointing toward innovation in large-area design of twisted heterostructures for their potential applications in quantum nanoelectronics, quantum photonics, optoelectronics, quantum computing, nonvolatile memory, quantum emission, and quantum communication. Moiré physics of moiré quantum materials is a relatively new and extremely exciting area of research. This article provides a general overview of recent advances of moiré physics in twisted van der Waals heterostructures of 2D materials.

**Keywords** 2D materials · Van der Waals heterostructures · Twisted bilayers · Moiré physics

## 1 Introduction

Years of research has shown that it is possible to alter the characteristics of a material by reducing its dimensions from three-dimension (3D) down to low-dimensional materials, i.e., bulk 3D graphite to either two-dimensional (2D) graphene, one-dimensional (1D) carbon nanotubes, or zero-dimensional (0D) fullerenes or quantum dots. In recent years, however, a new breakthrough was made in realizing that reducing the material dimensions is not the only way to coax a material into exhibiting new characteristics but so is the idea of twisting layered 2D materials [1, 2]. Twist is an additional degree of freedom that allows two layers of 2D materials to be twisted on top of one another to exhibit new properties that the materials would not have

✉ Sanjay K. Behura  
behuras@uapb.edu

<sup>1</sup> Department of Chemistry and Physics, University of Arkansas at Pine Bluff, 1200 N. University Drive, Pine Bluff, AR 71601, USA

<sup>2</sup> Department of Mathematics and Computer Science, University of Arkansas at Pine Bluff, 1200 N. University Drive, Pine Bluff, AR 71601, USA

<sup>3</sup> Department of Chemical Engineering, University of Illinois at Chicago, 929 W. Taylor Street, Chicago, IL 60607, USA

<sup>4</sup> Department of Chemistry, Physics and Atmospheric Sciences, Jackson State University, 1400 John R. Lynch Street, Jackson, MS 39217, USA

shown otherwise. Some of the more explored properties that have shown considerable deviation from expected outcomes include electronic, optical, and magnetic phenomena [3]. So what happens when the top monolayer of 2D crystal vertically stacked and rotated with a finite twist angle with respect to the bottom monolayer? Artificial moiré superlattices are created with the periodic moiré pattern that is found to control the interlayer hybridization resulting in strongly correlated quantum phases, which is otherwise not available in individual monolayers. For example, a monolayer graphene is a weakly interacting 2D electron system.

Among many recently developed exotic quantum phenomena found in the twisted heterostructures of 2D crystals, Fig. 1 presents some key findings in this area such as flat bands [4–13], interlayer ferromagnetism [14], moiré excitons [15–18], topological polaritons [19–21], soliton superlattices [22, 23], and interfacial superlattices [24–26]. In the process of exploring these new properties, creative techniques have been developed to design and visualize such moiré superlattices [3, 27, 28]. Furthermore, computational methods have also been explored in pursuit of accurately simulating the effects of twist angles on such quantum phenomena in moiré superlattices [29].

The area of twistorics is exploratory in nature; therefore, most research conducted thus far is a means of establishing the groundwork for this newly discovered field.

In this review article, we will discuss some emergent quantum phenomena in twisted bilayer heterostructures of 2D materials including (A) flat bands in the twisted bilayer graphene, (B) exciton superlattices in the twisted transition metal dichalcogenides (TMDs), (C) topological polaritons and photonic superlattices in the twisted 2D metal oxides, (D) interlayer magnetism in the stacked 2D magnetic semiconductors, and (E) unconventional ferroelectricity in moiré quantum materials. To thoroughly understand the moiré physics of the above quantum phenomena, this article will begin by presenting the fundamental concepts of van der Waals heterostructures and physics of moiré superlattices followed by a discussion on how to design and fabricate moiré quantum materials. The possible challenges with fabrication, characterization, and applications of twisted heterostructures are also highlighted. Few interesting quantum phenomena that will not be discussed in detail are soliton superlattices [22, 23] and interfacial superlattices [24–26] in twisted heterostructures

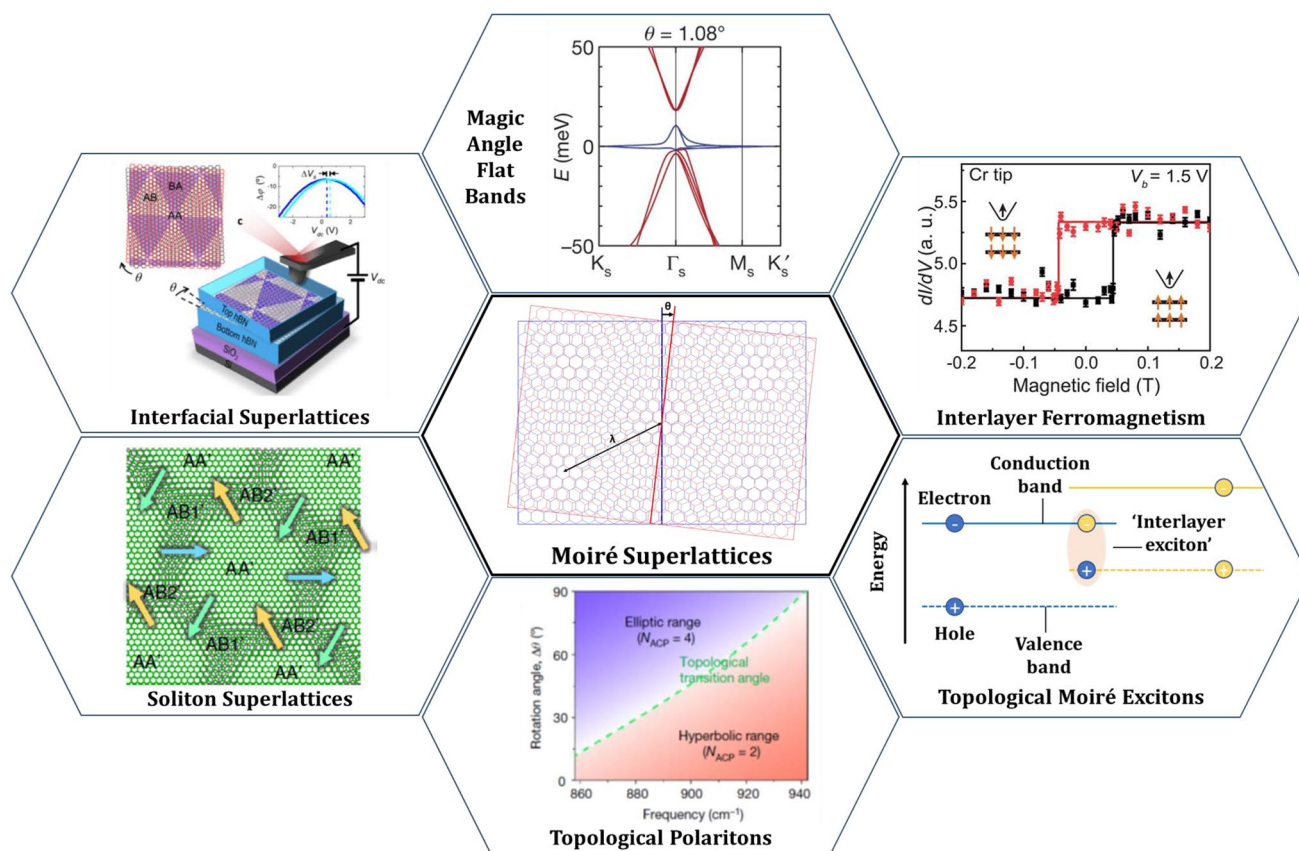


**Fig. 1** Emergent quantum phenomena in artificial moiré superlattices formed by vertically stacking two 2D monolayers and rotating one of the layers with a finite twist angle. Reproduced with permission from Refs. [4, 14, 19, 22, 24]

of polar van der Waals materials like hexagonal boron nitride (h-BN).

## 2 Van der Waals heterostructures and moiré superlattices

2D van der Waals heterostructures are artificial materials that are stacked layer by layer in a certain pattern and held together loosely by van der Waals forces [30, 31]. Covalent bonds allow the atoms within the plane to remain stable while the comparatively weaker van der Waals forces in between the layers hold the layers to be stacked vertically [32–34]. Every material is made up of repeating patterns of atoms referred to as a lattice. These lattices may be stacked in various patterns, the most common being AA-type stacking and AB-type stacking. AA-type stacking occurs when the lattice patterns align perfectly with one another while AB-type stacking involves the lattice being slightly offset from one another [35]. The choice in stacking configuration does change the properties of the material. This is because the stacking pattern of the layers alters the ability for electrons to transfer between layers.

Twistronics is the study of the twisted monolayers of 2D materials. In their bulk forms, materials like graphite and molybdenum disulfide ( $\text{MoS}_2$ ) are commonly used as dry lubricants. The reason being that weaker van der Waals forces between the layers make rotating or sliding layers a relatively easy task. When the same principle is applied to bilayer materials, the ability to rotate layers on top of one another opens doors for exciting new discoveries. When bilayers of material are rotated at a certain angle with respect to one another, then a more complex pattern of repetition is observed, called a superlattice. Rotating layers cause the stacking orders to differ; if the angle of rotation is in between AA and AB stacking, then a new pattern arises which is referred to as a moiré pattern (Fig. 2). This pattern is important when considering

electronic and mechanical properties due to it mimicking the well-known honeycomb structure that graphene is known for having, but on a larger scale which alters the interlayer hybridization. This moiré pattern has also been shown to create a fractal energy spectrum in a strong magnetic field [35]. The angle of rotation between layers plays an important role in determining which property changes will be observed. The properties observed at small angle twist can drastically differ from larger angles. Another factor that has shown to play a role in twisting properties is the doping of the material. Experiments have shown that the characteristics of the doped layers twisted at a certain angle can be very different from the non-doped layers twisted at the same angle. Thus far, it has been shown that twisting stacked layers on top of one another allows for unique characteristic changes in the materials's electronic, optical, and magnetic properties [3].

The twisted 2D monolayers form moiré superlattice with a moiré wavelength ( $\lambda$ ), which can be described as follows [3]:

$$\lambda = \frac{(1 + \delta)a_0}{\sqrt{2(1 + \delta)[1 - \cos\theta] + \delta^2}}$$

where  $\delta$  is the lattice mismatch between 2D monolayers, which can be presented as:  $\delta = \frac{|a'_0 - a_0|}{a_0}$ ;  $a_0$  and  $a'_0$  are the lattice constants of two 2D monolayers and  $\theta$  is the twist angle between the layers.

## 3 Design and fabrication of moiré quantum materials

Moiré quantum materials are twisted heterostructures in which atomically thin 2D materials are carefully stacked and rotated with a finite twist angle while the weak van der Waals force is responsible to hold the 2D layers. There are several techniques (as presented in Fig. 3) such as (i)

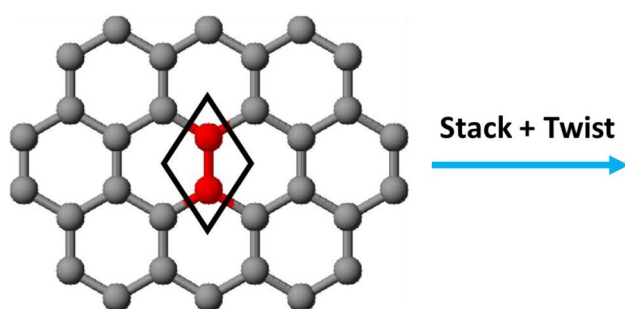
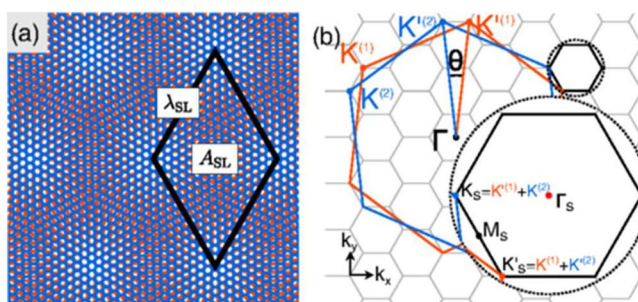


**Fig. 2** Transformation of a monolayer graphene via stacking of another monolayer graphene followed by a small angle-twist to a twisted bilayer graphene superlattice with moiré pattern that may host strongly correlated electronic states. The small-angle rotation leads



to the formation of a mini-Brillouin zone due the difference between the two K (or K') wavevectors for the two monolayers of graphene. Reproduced with permission from Ref. [52]

optical alignment of crystal edges [36–38], (ii) rotational alignment during assembly [39], (iii) self-rotation through thermal annealing [40, 41], and (iv) in situ rotation of 2D layers [3] that may be utilized when designing, for example, twisted graphene/h-BN heterostructures to be studied for twist-dependent quantum phenomena. These techniques have evolved since the initial discovery of moiré physics in twisted van der Waals heterostructures of 2D materials from only being able to allow for static analysis to allowing dynamic twist angle analysis.

A wide range of moiré materials have been developed from graphene, hexagonal boron nitride (h-BN), TMDs, or magnetic semiconductor crystals to exploit exotic quantum phenomena [42]. Such moiré quantum materials can be classified as (i) homobilayers—when two monolayers of same material are stacked with a twist angle (examples: twisted bilayer graphene, twisted TMD homobilayers), (ii) heterobilayers—when two monolayers of different materials with lattice mismatch are stacked and/or with a potential twist angle (examples: graphene/h-BN,  $\text{MoS}_2/\text{WS}_2$ ), and (iii) multilayers—when multiple layers of monolayers are stacked with a twist angle (examples: twisted double bilayer graphene, twisted double bilayer TMDs, twisted trilayer graphene). Therefore, the techniques to design and fabricate such wide varieties of moiré quantum materials may also vary.

#### 4 Emergence of exotic quantum phenomena in twisted bilayer heterostructures

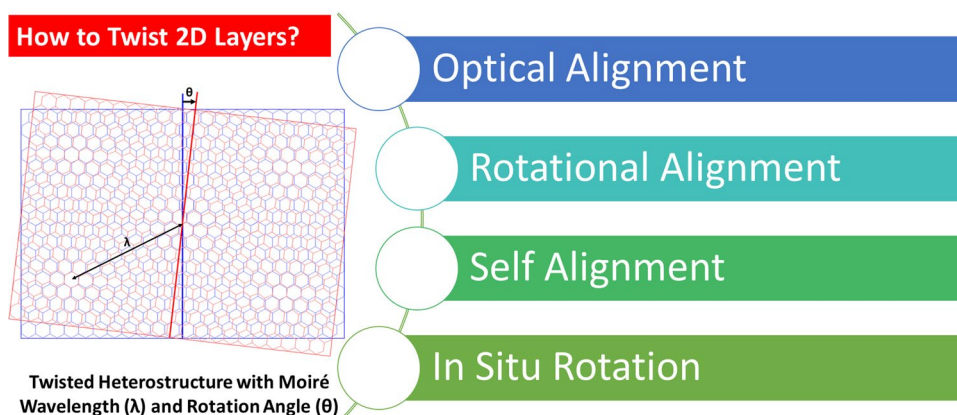
A slight lattice mismatch between the two 2D monolayers in a twisted heterostructure leads to the moiré pattern with the periodic length scale larger than that of lattice atoms of the individual layers. The moiré pattern is found to control the interlayer hybridization in a twisted bilayer heterostructure. Owing to the moiré pattern—introduced interlayer hybridization or coupling in twisted bilayer heterostructures, several exotic quantum phenomena in the broad area of nanoelectronics, excitonic science, magnetism, and photonics are

recently found in the engineered metamaterials with additional twist degree of freedom. Here we have discussed the most notable findings for twisted heterostructures of both homo- and heterobilayers of 2D materials including (A) flat bands, (B) exciton superlattices, (C) photonic superlattices, (D) interlayer magnetism, and (E) moiré ferroelectricity.

**A. Flat bands in twisted bilayers** The relationship between electron's energy and its momentum,  $E(k)$ , is known as the electronic band structure, which is key to predict the electron kinetics in a crystal. A crystal is defined as lattice + basis. In case of a 2D crystal lattice, for example, graphene, the block electrons are massless owing to the linearly dispersive energy bands [43]. Certain lattices (also known mathematically as “line graphs”) may also exhibit “flat bands” in their electronic band structure [43]. Flat band refers to zero-velocity points in momentum space of electrons near the Fermi level such that electron's kinetic energy is quenched and hence, Coulomb interactions are enhanced [43, 44]. Such strongly correlated electronic phases due to flat band formation in certain geometrically frustrated lattices [45] may give rise to emerging quantum phenomena such as superconductivity [46], itinerant ferromagnetism [47], and charge-density wave instability [48] and metal–insulator transition [49]. Figure 4A presents charge confinement and flat bands in kagome lattice and kagome metal CoSn [45].

Among various flat band systems that appear in bulk solids, we will now focus on creating the strongly correlated quantum phases in a magic angle twisted bilayer graphene superlattice (Fig. 4B) which also exhibits Mott-insulating phase and unconventional superconductivity [4, 50]. A periodic moiré pattern is constructed when a second layer of graphene is introduced and rotated at a small angle with respect to the first graphene layer [51]. This periodic moiré pattern extends throughout the superlattice and exhibits a strong localization of electronic wavefunctions at AA stacking domains. Figure 4B shows moiré patterns in twisted bilayer graphene with moiré wavelength ( $\lambda$ ) =  $a/[2\sin(\theta/2)]$ , where  $a = 0.246$  nm is the lattice constant of graphene and

**Fig. 3** Fabrication methods for the design of moiré quantum materials including twisted graphene/h-BN heterostructures





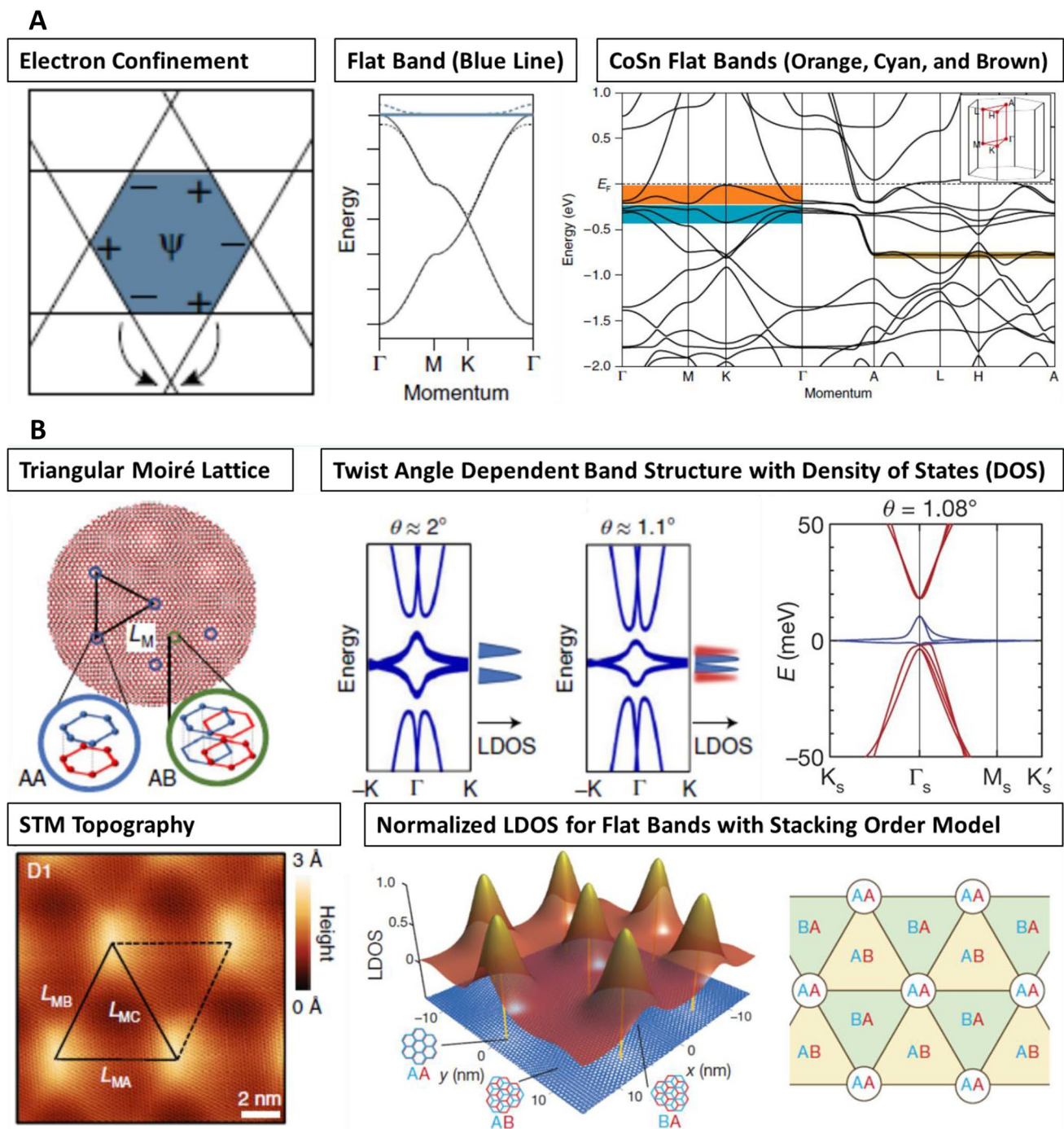


**Fig. 4** **A** Charge confinement and flat bands in kagome lattice and kagome metal CoSn. **B** Twisted bilayer graphene system: moiré superlattice with AA and AB stacking, band energies, STM topogra-

phy, normalized LDOS, and stacking order model. Reproduced with permission from Refs. [4, 45, 51]

$\theta$  is the twist angle. Figure 4B depicts the twisted bilayer graphene system with moiré superlattice of AA and AB stacking, band energies with flat bands based on ab initio tight-binding method, STM topography of moiré superlattice,

local density of states (LDOS) corresponding to flat bands, and stacking order model.

A 2016 report by Cao et al. [52] studies the magnetotransport properties of twisted bilayer graphene which provides promise for further investigation. A more recent

paper by Cao et al. [4] extends the study of van der Waals heterostructures to include bilayer graphene to show that twisting the layers a “magic angle” of 1.1 degrees allows for flattened electronic bands. These bands exhibit Mott-like insulator states when half-filled. The paper poses that continued research of twisted bilayer graphene may open many doors to the mysterious world of many body quantum phases. Upon further investigation of twisted bilayer graphene “magic angle,” Cao et al. [50] was able to develop a superconductor with some of the strongest observable pairing strength between electrons. They show measurements of twisted bilayer graphene having comparable features to cuprates by electrostatic doping the previously observed Mott-like insulating states. In response to the discovery of superconductivity in twisted bilayer graphene, Laksono et al. [53] followed up with a model that predicts multiple combinations of insulating and superconducting phases.

Though this phenomenon is still relatively new, there have been a considerable amount of attention given to twisted bilayer graphene and little to other heterostructures. Another recent study [54] has crossed that bridge and has applied first principles density functional theory to calculate the electronic and structural transformations in twisted bilayer molybdenum disulfide ( $\text{MoS}_2$ ).  $\text{MoS}_2$  has structural differences compared to graphene but when considering twisted layers, the two materials have comparable flat band bandwidths which can influence the electronic structure in the observed moiré patterns similar to the effects seen in graphene. It has also been found that doping these flat bands in  $\text{MoS}_2$  may lead to transitions between states depending on the amount of filling, similar to the way twisted bilayer graphene becomes a Mott insulator at half-filling.

**B. The influence of moiré potentials on excitons in twisted bilayer heterostructures** Three-atom-thick TMDs such as  $\text{MoS}_2$ ,  $\text{WS}_2$ ,  $\text{MoSe}_2$ , and  $\text{WSe}_2$  are a class of layered 2D crystals with weak interlayer van der Waals bonding and strong intralayer covalent bonding [55, 56]. Owing to the van Hove singularity induced strong optical absorption and exciton generation in the visible part of the electromagnetic spectrum, TMDs are suitable for strong light-matter interactions in optoelectronic devices [57, 58].

The twisting of vertically stacked 2D layers of TMDs forms periodic energy potentials referred to as moiré potentials [59]. The influence of the moiré potentials on excitons formed by type-II band alignment in twisted bilayer TMD heterostructures results in interesting opto-electrical and topographical changes [60–62]. Diffusion of excitons can take place either in a single layer (intralayer exciton diffusion) or between bilayers of TMDs (interlayer exciton diffusion) [63]. The interaction of an excitons’ electron and hole, generated via optical absorption, forms a valley pseudospin. The valley pseudospins of excitons observed in twisted TMDs

have longer lifetimes when involving interlayer excitons [64, 65] as opposed to intralayer excitons. The longer lifetimes make interlayer excitons more efficient information carriers compared to short-lived excitons [66]. This emerging phenomenon paves the way for new electronics as the tuning of excitons via twisting bilayers proves to be a valuable tool in the field of solid-state quantum information technology.

Choi et al. observed that interlayer exciton lifetimes are temperature dependent with different twist angles [60]. The dependence on twist angle originates from the spacing between the electron and hole. The lifetime of interlayer excitons increases as the conduction band minimum is twisted away from the valence band maximum. In doing this, the interlayer exciton also experiences a decreasing dipole moment resulting in decreasing emission intensity [61]. When moiré potentials are introduced to interlayer excitons, the excitons experience localization which leads to new optical selection rules at three-fold symmetry sites or slow the diffusion process [61]. This is because the spin-singlet and spin-triplet can couple to in- and out-of-plane polarized light making them equally bright in measurements while at three-fold symmetry sites. Bilayer heterostructures such as h-BN-encapsulated  $\text{MoSe}_2$ - $\text{WSe}_2$  at low temperatures and h-BN-encapsulated  $\text{WS}_2$ - $\text{WSe}_2$  at near  $0^\circ$  twist angle reported multiple interlayer exciton resonances in photoluminescence measurements for both ground and excited states that further prove the alternating selection rules.

Alternatively, the moiré potential impact on intralayer excitons is smaller than that of interlayer excitons. However, it is still possible to tune the energy spacing and oscillator strength of resonances by twisting the bilayer heterostructure. In this case, a valley of pseudospin with a momentum-space Berry phase, when in combination with a moiré potential and a Zeeman field, leads to the transport of excitons along the edge states [59, 62]. Despite the changes in twist angles, the selection rules remain the same making intralayer excitons coupled to light. When coupling optical and electrical fields, proportionality has been observed between the density of states of moiré potentials and changes in the induced optical contrast of  $\text{WSe}_2$  intralayer resonance giving rise to insulating states at certain densities [61].

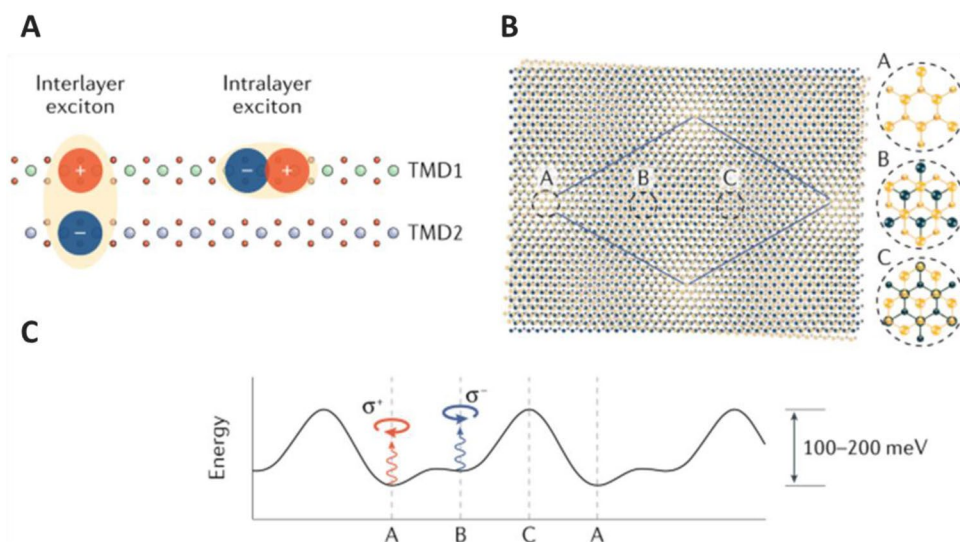
In some studies, hybridized excitons [67] have been observed to be tunable by both electrical and optical fields. These occur when optical oscillations are transferred from intralayer excitons to degenerate interlayer excitons while sharing electron or hole states. Complications in determining exciton delocalization exist due to the differences in the orbital natures of the two component layers present in bilayer heterostructures [61]. Figure 5 presents interlayer and intralayer excitons in twisted TMD heterostructure with corresponding moiré potential energy at different stacking regions.

**C. Photonic superlattices in twisted heterostructures** Development in photonics is not far behind than the exotic electronic quantum phenomena that we discussed in the context of twisted bilayer heterostructures. Like electronic properties are dependent on twisted lattices of 2D crystals, photonic behavior also changes with twist degrees of freedom. Quantum photonic phenomena are observed not only in isolated 2D crystals but also in van der Waals heterostructures. These are including surface plasmon polaritons (SPPs) in graphene [68], surface phonon polaritons in hexagonal boron nitride (h-BN) [69–72], tunable plasmon–phonon polaritons in graphene-h-BN heterostructures [73], and surface exciton polaritons in transition metal dichalcogenides [74–78]. It will be interesting to see if further engineering the 2D van der Waals heterostructures via twisting one of the layers will have any effect on the polariton physics.

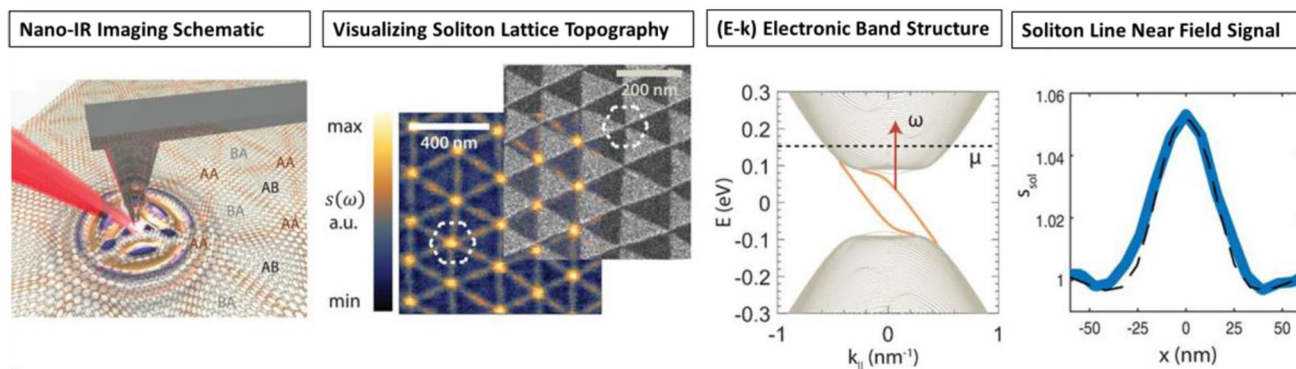
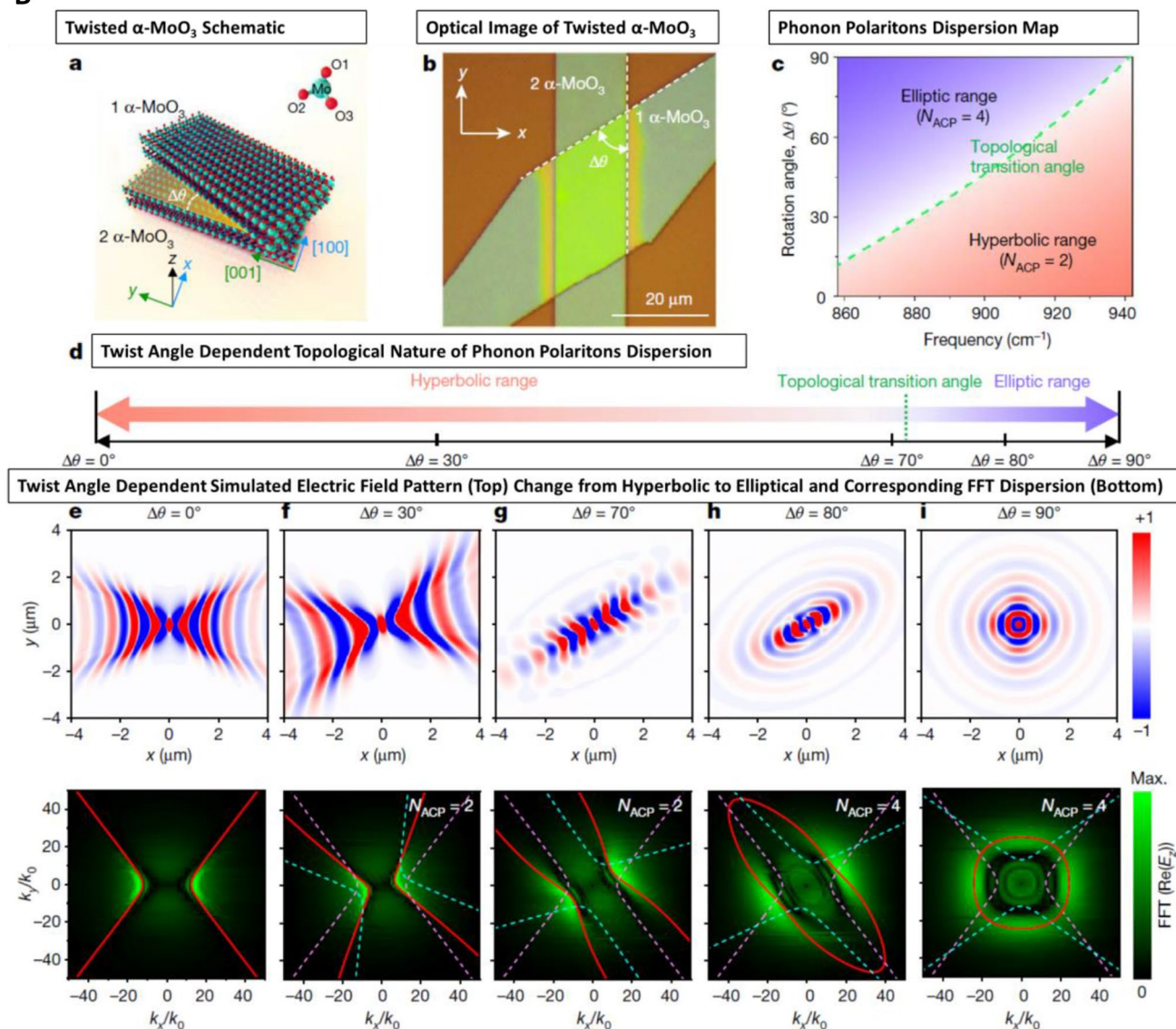
Moiré patterns in twisted bilayer graphene results into the flat band–induced transition of Mott insulator to superconducting phases owing to the interlayer-hybridized strongly correlated electrons. Similar to quantum electronic transport in the twisted bilayer graphene-based moiré superlattices, surface plasmons, a collective oscillations of photon and graphene plasmon, can also be controlled with confined propagation in the periodic superlattice structures [21, 79]. To understand the propagation of SPPs in twisted bilayer graphene, it is critical to look at the periodic superlattice structure of twisted bilayer graphene with small angle. TBG exhibits triangular moiré lattice with commensurate AA domains having large density of states and the spatial period is separated by the incommensurate AB and BA triangular domains (as shown in Fig. 6A) [23, 51, 79]. Therefore, strength of electronic correlations or periodic potentials spatially varies across the moiré lattice of twisted bilayer graphene as well as at moiré domain walls called “solitons” (as shown in Fig. 6A). Twisted bilayer graphene

system provides a unique photonic crystal platform to study SPPs without depending on complex lithography processing. This is because the twisted bilayer graphene produces soliton lattice (periodic pattern of solitons) which behaves as periodic array of scatterers to manipulate graphene plasmons [79]. Such soliton superlattices are also observed in twisted h-BNs using nano-IR spectroscopy [22]. Yet another promising discovery for nanophotonics shows that adjusting the angle between twisted bilayer graphene results in measurable differences in plasmon wavelengths [80]. F. Hu et al. [80] present a method to observe plasmonic behavior in twisted bilayer graphene through the use of a scattering-type scanning near-field optical microscope as well as a numerical model, dubbed the spheroid model, that can be used to quantify such behavior. By analyzing the near-field scattering amplitude and phase at varying angles, it was concluded that twisted bilayer graphene does support infrared plasmons in the Dirac linear regime. Additionally, the study shows that the spheroid model proved to be accurate for twist angles greater than  $3^\circ$  since lower twist angles in bilayer graphene exhibit flat bands which deviate from the Dirac approximation. Plasmonic studies may benefit greatly with further investigation of adjustable parameters in twisted bilayer materials. In contrast to the study of phonon polaritons in polar van der Waals materials, there has been recent report on emergence of phonon polaritons in twisted bilayers of  $\alpha$ -phase molybdenum trioxide ( $\alpha$ -MoO<sub>3</sub>) [19] as shown in Fig. 6B. Here phonon polariton dispersion has been observed to make tunable transition from hyperbolic to elliptical dispersion contours, which are due to the interlayer polariton hybridization analogous to the twisted bilayer graphene-based interlayer hybridization-induced flat band system [19].

**Fig. 5** **A** Interlayer and intra-layer excitons in **B** twisted transition metal dichalcogenide heterostructure with **C** corresponding moiré potential energy at different stacking regions. Reproduced with permission from Ref. [63]





**A****B**

**Fig. 6** Photonic superlattices in twisted bilayers. **A** Nano-light photonic crystal formed by a network of solitons in twisted bilayer graphene. **B** Rotation-induced topological transition of phonon polaritons in twisted bilayer  $\alpha\text{-MoO}_3$ . Reproduced with permission from Refs. [19, 79]



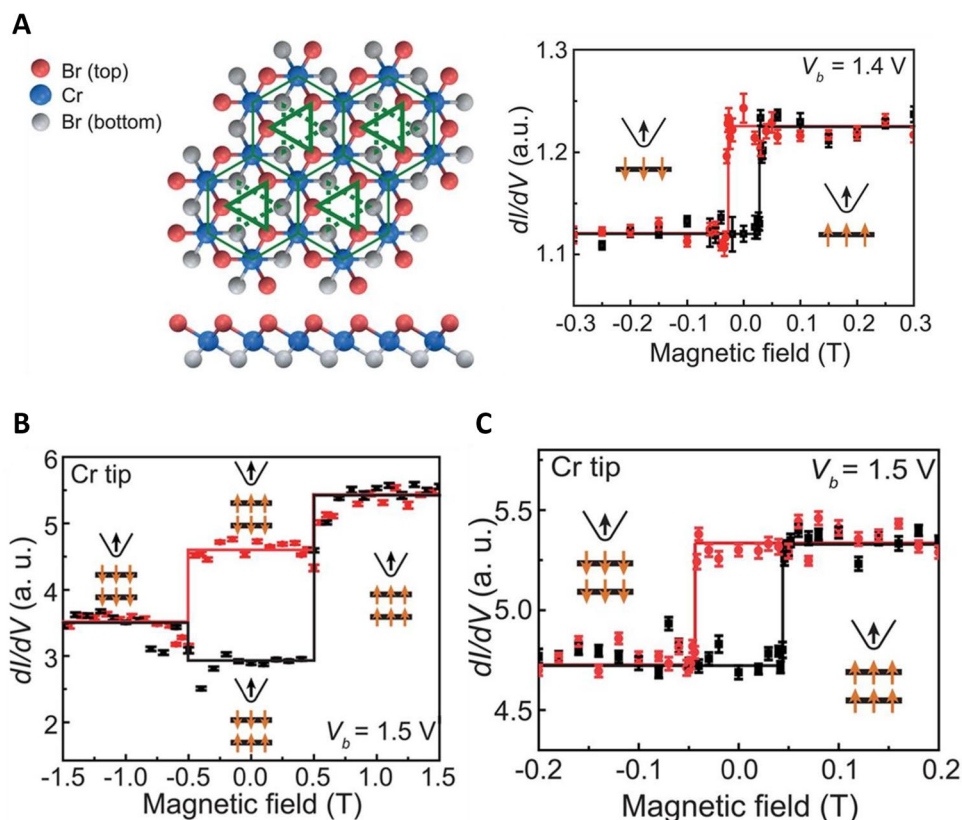
**D. Interlayer magnetism in twisted magnetic semiconductors** By now, we have seen that the twisted bilayers of 2D nanomaterials have unique physics to offer in the context of electrical and optical properties. This is because of the strong electronic and optoelectronic interlayer coupling. The magnetic properties are observed in atomically thin 2D materials, specifically chromium trihalide,  $\text{CrX}_3$  ( $\text{X} = \text{Cl}, \text{Br}, \text{I}$ ) family [81, 82]. It has recently been observed that van der Waals bilayer materials exhibit interlayer magnetic coupling, which are dependent on stacking order through rotation and translation between the layers [14], thus opening a new direction to investigate. A 2015 report on bulk layered  $\text{CrI}_3$  depicted temperature-dependent structural phase transition from rhombohedral at low temperature to monoclinic at high temperature [83].

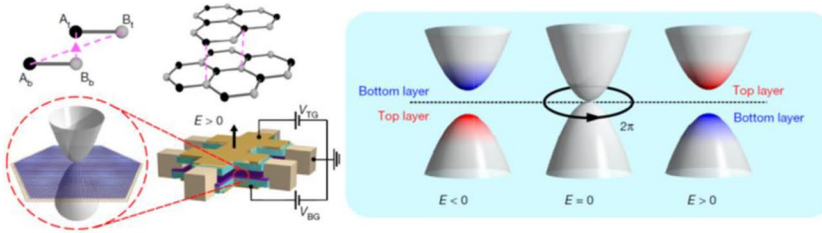
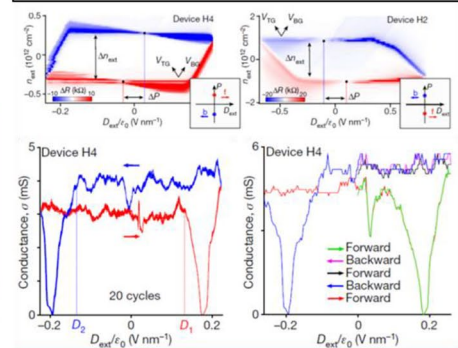
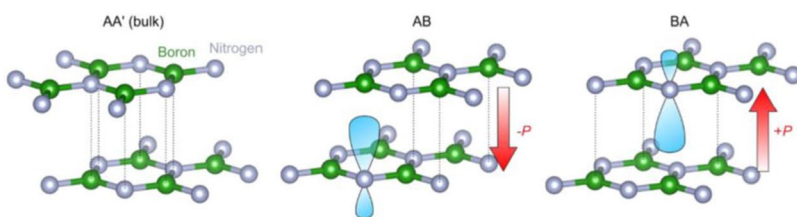
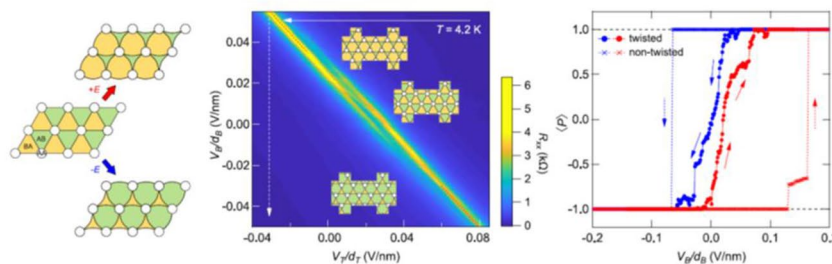
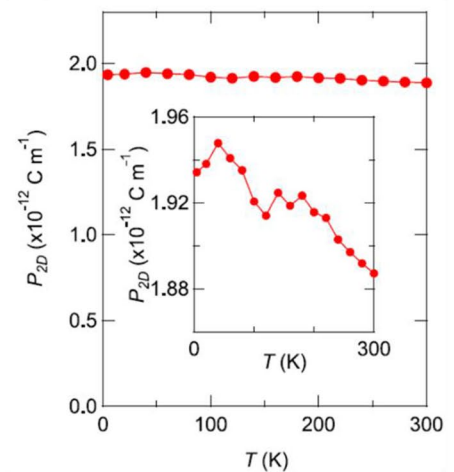
This phenomena provided evidence to study the correlation between crystal structure and magnetic properties with a possibility of finding magnetism in 2D form [83]. Indeed recent experiments revealed interesting magnetic phenomena including ferromagnetism in the monolayer  $\text{CrI}_3$  and interlayer antiferromagnetism in its bilayer form [14]. Another sister compound material in the chromium trihalide family,  $\text{CrBr}_3$ , shows ferromagnetic interlayer coupling observed via polar reflectance magnetic circular dichroism [84]. Figure 7A: left panel shows the crystal structure (top and side views) of monolayer  $\text{CrBr}_3$  in which Cr atoms are

arranged in a honeycomb lattice surrounded by Br atoms from top and bottom [14]. The corresponding magnetic hysteresis is presented in Fig. 7A: right panel for a monolayer  $\text{CrBr}_3$ . In contrast, to study the interlayer magnetic coupling in a bilayer  $\text{CrBr}_3$  crystal, two-stacking geometry such as R-type and H-type is considered by Chen et al. [14]. If both top and bottom layers in  $\text{CrBr}_3$  are aligned in the same orientation, it corresponds to R-type stacking order. In contrast, if both top and bottom layers are of  $180^\circ$  orientation, it corresponds to the H-type stacking. The R-type and H-type stackings exhibit interlayer antiferromagnetic and ferromagnetic coupling as presented in Fig. 7B and C measured via in situ spin-polarized scanning tunneling microscopy and spectroscopy [14]. Figure 7 presents crystal structure of monolayer  $\text{CrBr}_3$  and corresponding magnetic hysteresis, interlayer antiferromagnetic coupling in an R-type stacked bilayer  $\text{CrBr}_3$ , and interlayer ferromagnetic coupling in an H-type stacked bilayer  $\text{CrBr}_3$ .

**E. Ferroelectricity in moiré quantum materials** Ferroelectric materials exhibit spontaneous polarization (formation of electric dipoles through separation of +ve and -ve charge centers) even without the application of an external electric field. Such a polarization can be switchable by applying a strong electric field in a ferroelectric material. Owing to the intrinsic remnant and switchable polarization characteristics,

**Fig. 7** **A** Crystal structure of monolayer  $\text{CrBr}_3$  and corresponding magnetic hysteresis. **B** Interlayer antiferromagnetic coupling in an R-type stacked bilayer  $\text{CrBr}_3$ . **C** Interlayer ferromagnetic coupling in an H-type stacked bilayer  $\text{CrBr}_3$ . Reproduced with permission from Ref. [14]



**A****A-1: Bernal Stacked Bilayer Graphene (BLG): Lattice, Band Dispersion and Layer Polarization, and Device Architecture with Moiré Superlattice****A-2: Polarization and FE Switching****B****B-1: Atomic Arrangements of AA' (Bulk) and AB and BA Stacked h-BN****B-2: Switching of Ferroelectric Response in Twisted h-BN Crystals****B-3: Temperature-dependence Study of Ferroelectricity in Stacked Bilayer h-BN**

**Fig. 8** **A** Ferroelectricity in Bernal stacked bilayer graphene/boron nitride moiré system. **B** Ferroelectric response in AB stacked bilayer hexagonal boron nitride. Reproduced with permission from Refs. [91, 92]

ferroelectric materials are suitable for advanced electronics and energy applications such as nonvolatile memory [85], neuromorphic computing [86], and solar cells [87]. Ferroelectric phenomenon is observed not only in bulk materials with noncentrosymmetric structure but also in thin films of few nanometers and even down to unit cells [88–90]. Many 2D nanomaterials with high polarizability or noncentrosymmetric structures have shown ferroelectric response as observed via experimental or theoretical studies. Few examples include 1 T MoS<sub>2</sub>, 1 T MoTe<sub>2</sub>, GeSe, and In<sub>2</sub>Se<sub>3</sub>.

Here we will discuss the signature of ferroelectric phenomena in moiré quantum materials such as Bernal stacked bilayer graphene and AB stacked bilayer h-BN [91, 92]. This is because these engineered moiré quantum heterostructures

are seen to exhibit strong electronic correlations and spontaneous symmetry breaking, which are prerequisites for the ferroelectricity in low-dimensional systems. Zheng et al. showed switchable ferroelectricity in Bernal stacked bilayer graphene sandwiched between two hexagonal boron nitride layers [91]. Figure 8A displays the ferroelectric response in Bernal stacked bilayer graphene/boron nitride moiré system. The lattice structure of Bernal stacked BLG system, energy band dispersion as a function of vertical electric field, and BN-encapsulated BLG with moiré superlattice pattern are presented in Fig. 8A-1. The electric polarization and ferroelectric switching are also depicted in Fig. 8A-2. Ferroelectric response is also observed in AB stacked h-BN as reported recently by Yasuda et al. [92]. Figure 8B displays

the ferroelectric response in AB stacked h-BN. The arrangements of boron and nitrogen atoms in AA' (bulk structure of h-BN), and AB as well as BA stacked h-BN crystals with possible polarization are schematically presented in Fig. 8B-1. The ferroelectric switching as a function of vertical electric fields is shown in Fig. 8B-2. Figure 8B-3 presents the temperature dependence of ferroelectricity in stacked bilayer h-BN system.

## 5 Challenges with design, characterization, and applications of moiré quantum materials

The area of moiré physics and moiré quantum materials is still a very new and promising field of research with many possibilities still untouched. However, there exists acute challenges in design, characterization, and applications of moiré quantum materials. First, the stability of some of the 2D crystals needs to be investigated through interfacial engineering or encapsulated method without affecting the twisted heterostructures. For example, the 2D magnetic materials [93–95] and their stacked/twisted topology possess excellent platform for advanced spintronic applications; it is also critical to realize that 2D magnetic materials are unstable in ambient conditions. Several methods have also been developed to stabilize the air-sensitive 2D magnetic materials including (i) atomic layer deposited ultrathin MgO passivation layer on CrBr<sub>3</sub> magnetic materials [96] and (ii) isolating air stable 2D Ta<sub>3</sub>FeS<sub>6</sub> magnetic material with intrinsic long-range ferromagnetic order [97]. Second, there are major challenges in designing large-area twisted heterostructures of 2D crystals without using any transfer-related steps. Most of the twisted heterostructures are through mechanical exfoliation and stacking approach. The ability to in situ control the small angle twist of two 2D materials while visualizing the moiré superlattices and measuring the quantum phenomena will be a major step ahead in area of moiré physics and moiré quantum materials [98]. The role of defects, strain, edges in 2D crystals on twisted superlattice architecture, and associated quantum phenomena will be interesting to study. Third, the structural, optical, and electronic characterization of moiré superlattices to explore strongly correlated physics is strictly limited to sophisticated tools and analysis. Fourth, the integration of moiré quantum materials in electronic or quantum photonic circuits will multiply their functionalities, but a great deal of research is essential to achieve this. Furthermore, 3D metal contacts to 2D twisted heterostructures (moiré quantum materials) as well as the contact geometry and interfacing may sacrifice the carrier transport and dynamics in the moiré quantum material devices. Exploring the contact topology

and interfacial engineering to the moiré quantum material devices will benefit their applications [99, 100].

## 6 Opportunities and outlook

Moiré physics based on twisted van der Waals heterostructures of 2D quantum materials is a new and promising area of research with multitude of possibly unknown properties and phenomena. The ability to isolate, stack, and dynamically rotate a wider range of 2D crystals and scaling fabrication methods may lead to exciting new technological applications in nanoelectronics, photonics, optoelectronics, quantum computing, nonvolatile memory, quantum emission, and communication. Here we have discussed some emergent quantum phenomena found in moiré superlattices of 2D crystals. Unconventional superconductivity and resonant tunneling are among many exciting new properties also observed in van der Waals 2D heterostructures with twist degree of freedom. Many mysteries still cloud the topic of moiré physics that may be answered by further research and development on twisted bilayers or trilayers or multilayers. We envision that the area of moiré materials and moiré physics requires some key developments in superlattice growth, in situ twist control, and stability of materials and devices. These include (i) development in design of large-area moiré superlattices via transfer-free direct growth through chemical vapor deposition, (ii) in situ control of twist angles during property measurements at extreme conditions, and (iii) strategies for crystal stability of certain 2D magnetic materials and stacked/twisted devices.

**Acknowledgements** SKB acknowledges the support from the Department of Chemistry and Physics and the Department of Mathematics and Computer Science at the University of Arkansas at Pine Bluff. NRP acknowledges the funding support from NSF-PREM through NSF DMR # 1826886.

## Declarations

**Conflict of interest** The authors declare no competing interests.

## References

1. E. Y. Andrei and A. H. MacDonald. Graphene bilayers with a twist. *Nature Materials* **19**, 1265–1275 (2020). <https://doi.org/10.1038/s41563-020-00840-0>
2. A. H. MacDonald, Bilayer Graphene's Wicked, Twisted Road. *Physics* **12**, 12 (2019). <https://doi.org/10.1103/physics.12.12>
3. R. Ribeiro-Palau, C. Zhang, K. Watanabe, T. Taniguchi, J. Hone, and C. R. Dean, Twistable electronics with dynamically rotatable



- heterostructures. *Science* **361**(6403), 690–693 (2018). <https://doi.org/10.1126/science.aat6981>
4. Y. Cao, V. Fatemi, A. Demir, S. Fang, S. L. Tomarken, J. Y. Luo, J. D. Sanchez-Yamagishi, K. Watanabe, T. Taniguchi, E. Kaxiras, R. C. Ashoori, and P. Jarillo-Herrero. *Nature*, **556**, 80–84 (2018). <https://doi.org/10.1038/nature26154>
  5. E. Suárez Morell, J. D. Correa, P. Vargas, M. Pacheco, and Z. Barticevic, Flat bands in slightly twisted bilayer graphene: Tight-binding calculations. *Phys Rev B*, **82**, 121407(R) (2010). <https://doi.org/10.1103/PhysRevB.82.121407>
  6. Y. H. Zhang, D. Mao, Y. Cao, P. Jarillo-Herrero, and T. Senthil, Nearly flat Chern bands in moiré superlattices, *Phys. Rev. B*, **99**, 075127 (2019). <https://doi.org/10.1103/PhysRevB.99.075127>
  7. Z. Bi, N. F. Q. Yuan, and L. Fu, Designing flat bands by strain, *Phys. Rev. B*, **100**, 035448 (2019). <https://doi.org/10.1103/PhysRevB.100.035448>
  8. Balents, L.; Dean, C. R.; Efetov, D. K.; Young, A. F. Superconductivity and Strong Correlations in Moiré Flat Bands. *Nature Physics*, **16**, 725–733 (2020). <https://doi.org/10.1038/s41567-020-0906-9>
  9. Zhang, Z.; Wang, Y.; Watanabe, K.; Taniguchi, T.; Ueno, K.; Tutuc, E.; LeRoy, B. J. Flat Bands in Twisted Bilayer Transition Metal Dichalcogenides. *Nature Physics*, **16**, 1093–1096 (2020). <https://doi.org/10.1038/s41567-020-0958-x>
  10. Haddadi, F.; Wu, Q. S.; Kruchkov, A. J.; Yazyev, O. V. Moiré Flat Bands in Twisted Double Bilayer Graphene. *Nano Lett*, **20**, 2410–2415 (2020). <https://doi.org/10.1021/acs.nanolett.9b05117>
  11. Chebrolu, N. R.; Chittari, B. L.; Jung, J. Flat Bands in Twisted Double Bilayer Graphene. *Phys. Rev. B*, **99**, 235417 (2019). <https://doi.org/10.1103/PhysRevB.99.235417>
  12. Bistritzer, R.; MacDonald, A. H. Moiré Bands in Twisted Double-Layer Graphene. *Proc. Natl. Acad. Sci*, **108**, 12233–12237 (2011). <https://doi.org/10.1073/pnas.1108174108>
  13. Lisi, S.; Lu, X.; Benschop, T.; de Jong, T. A.; Stepanov, P.; Duran, J. R.; Margot, F.; Cucchi, I.; Cappelli, E.; Hunter, A.; Tamai, A.; Kandyba, V.; Giampietri, A.; Barinov, A.; Jobst, J.; Stalman, V.; Leeuwenhoek, M.; Watanabe, K.; Taniguchi, T.; Rademaker, L.; van der Molen, S. J.; Allan, M. P.; Efetov, D. K.; Baumberger, F. Observation of Flat Bands in Twisted Bilayer Graphene. *Nature Physics*, **17**, 189–193 (2021). <https://doi.org/10.1038/s41567-020-01041-x>
  14. Chen, W.; Sun, Z.; Wang, Z.; Gu, L.; Xu, X.; Wu, S.; Gao, C. Direct Observation of van Der Waals Stacking-Dependent Interlayer Magnetism. *Science*, 366(6468), 983–987 (2019). <https://doi.org/10.1126/science.aav1937>
  15. Zhang, L.; Zhang, Z.; Wu, F.; Wang, D.; Gogna, R.; Hou, S.; Watanabe, K.; Taniguchi, T.; Kulkarni, K.; Kuo, T.; Forrest, S. R.; Deng, H. Twist-Angle Dependence of Moiré Excitons in WS<sub>2</sub>/MoSe<sub>2</sub> Heterobilayers. *Nature Communications*, **11**, Article number: 5888 (2020). <https://doi.org/10.1038/s41467-020-19466-6>
  16. Guo, H.; Zhang, X.; Lu, G. Shedding Light on Moiré Excitons: A First-Principles Perspective. *Sci. Adv*, **6**(42), eabc5638 (2020). <https://doi.org/10.1126/sciadv.abc5638>
  17. Jin, C.; Regan, E. C.; Yan, A.; Iqbal Bakti Utama, M.; Wang, D.; Zhao, S.; Qin, Y.; Yang, S.; Zheng, Z.; Shi, S.; Watanabe, K.; Taniguchi, T.; Tongay, S.; Zettl, A.; Wang, F. Observation of Moiré Excitons in WSe<sub>2</sub>/WS<sub>2</sub> Heterostructure Superlattices. *Nature*, **567**, 76–80 (2019). <https://doi.org/10.1038/s41586-019-0976-y>
  18. Tran, K.; Choi, J.; Singh, A. Moiré and beyond in Transition Metal Dichalcogenide Twisted Bilayers. *2D Materials*, **8**(2), 022002 (2021). <https://doi.org/10.1088/2053-1583/abd3e7>
  19. Hu, G.; Ou, Q.; Si, G.; Wu, Y.; Wu, J.; Dai, Z.; Krasnok, A.; Mazon, Y.; Zhang, Q.; Bao, Q.; Qiu, C. W.; Alù, A. Topological Polaritons and Photonic Magic Angles in Twisted  $\alpha$ -MoO<sub>3</sub> Bilayers. *Nature*, **582**, 209–213 (2020). <https://doi.org/10.1038/s41586-020-2359-9>
  20. Chen, M.; Lin, X.; Dinh, T. H.; Zheng, Z.; Shen, J.; Ma, Q.; Chen, H.; Jarillo-Herrero, P.; Dai, S. Configurable Phonon Polaritons in Twisted  $\alpha$ -MoO<sub>3</sub>. *Nature Materials*, **19**, 1307–1311 (2020). <https://doi.org/10.1038/s41563-020-0732-6>
  21. Ni, G. X.; Wang, H.; Wu, J. S.; Fei, Z.; Goldflam, M. D.; Keilmann, F.; Özyilmaz, B.; Castro Neto, A. H.; Xie, X. M.; Fogler, M. M.; Basov, D. N. Plasmons in Graphene Moiré Superlattices. *Nature Materials*, **14**, 1217–1222 (2015). <https://doi.org/10.1038/nmat4425>
  22. Ni, G. X.; Wang, H.; Jiang, B. Y.; Chen, L. X.; Du, Y.; Sun, Z. Y.; Goldflam, M. D.; Frenzel, A. J.; Xie, X. M.; Fogler, M. M.; Basov, D. N. Soliton Superlattices in Twisted Hexagonal Boron Nitride. *Nature Communications*, **10**, Article number: 4360 (2019). <https://doi.org/10.1038/s41467-019-12327-x>
  23. Alden, J. S.; Tsen, A. W.; Huang, P. Y.; Hovden, R.; Brown, L.; Park, J.; Muller, D. A.; McEuen, P. L. Strain Solitons and Topological Defects in Bilayer Graphene. *PNAS*, **110**(28), 11256–11260 (2013). <https://doi.org/10.1073/pnas.1309394110>
  24. Woods, C. R.; Ares, P.; Nevison-Andrews, H.; Holwill, M. J.; Fabregas, R.; Guinea, F.; Geim, A. K.; Novoselov, K. S.; Walet, N. R.; Fumagalli, L. Charge-Polarized Interfacial Superlattices in Marginally Twisted Hexagonal Boron Nitride. *Nature Communications*, **12**, Article number: 347 (2021). <https://doi.org/10.1038/s41467-020-20667-2>
  25. Stern, M. V.; Waschitz, Y.; Cao, W.; Nevo, I.; Watanabe, K.; Taniguchi, T.; Sela, E.; Urbakh, M.; Hod, O.; Shalom, M. Ben. Interfacial Ferroelectricity by van Der Waals Sliding. *Science*, **372**(6549), 1462–1466 (2021). <https://doi.org/10.1126/science.abe8177>
  26. P. Zhao, C. Xiao, and Wang Yao, Universal superlattice potential for 2D materials from twisted interface inside h-BN substrate, *npj 2D Materials and Applications*, **5**, Article number: 38 (2021). <https://doi.org/10.1038/s41699-021-00221-4>
  27. Cui, X.; Sun, L.; Zeng, Y.; Hao, Y.; Liu, Y.; Wang, D.; Yi, Y.; Loh, K. P.; Zheng, J.; Liu, Y. Visualization of Crystallographic Orientation and Twist Angles in Two-Dimensional Crystals with an Optical Microscope. *Nano Lett*, **20**, 6059–6066 (2020). <https://doi.org/10.1021/acs.nanolett.0c02098>
  28. Luo, Y.; Engelke, R.; Mattheakis, M.; Tamagnone, M.; Carr, S.; Watanabe, K.; Taniguchi, T.; Kaxiras, E.; Kim, P.; Wilson, W. L. In Situ Nanoscale Imaging of Moiré Superlattices in Twisted van Der Waals Heterostructures. *Nature Communications*, **11**, Article number: 4209 (2020). <https://doi.org/10.1038/s41467-020-18109-0>
  29. Carr, S.; Massatt, D.; Fang, S.; Cazeaux, P.; Luskin, M.; Kaxiras, E. Twistronics: Manipulating the Electronic Properties of Two-Dimensional Layered Structures through Their Twist Angle. *Phys. Rev. B*, **95**, 075420 (2017). <https://doi.org/10.1103/PhysRevB.95.075420>
  30. S. Behura, P. Nguyen, S. Che, R. Debbarma, V. Berry, *J. Am. Chem. Soc.* **137**, 13060 (2015)
  31. Behura, S.; Nguyen, P.; Debbarma, R.; Che, S.; Seacrist, M. R.; Berry, V. Chemical Interaction-Guided, Metal-Free Growth of Large-Area Hexagonal Boron Nitride on Silicon-Based Substrates. *ACS Nano*, **11**, 4985–4994 (2017). <https://doi.org/10.1021/acs.nano.7b01666>
  32. Geim, A. K.; Grigorieva, I. V. Van Der Waals Heterostructures. *Nature*, **499**, 419–425 (2013). <https://doi.org/10.1038/nature12385>
  33. Novoselov, K. S.; Mishchenko, A.; Carvalho, A.; Castro Neto, A. H. 2D Materials and van Der Waals Heterostructures. *Science*, **353**(6298), aac9439 (2016). <https://doi.org/10.1126/science.aac9439>

34. Liu, Y.; Weiss, N. O.; Duan, X.; Cheng, H. C.; Huang, Y.; Duan, X. Van Der Waals Heterostructures and Devices. *Nature Reviews Materials*, **1**, Article number: 16042 (2016). <https://doi.org/10.1038/natrevmats.2016.42>
35. Rode, J. C.; Smirnov, D.; Belke, C.; Schmidt, H.; Haug, R. J. Twisted Bilayer Graphene: Interlayer Configuration and Magnetotransport Signatures. *Ann. Phys.*, **529**(11) (2017). <https://doi.org/10.1002/andp.201700025>
36. M. Yankowitz, J. Xue, D. Cormode, J.D. Sanchez-Yamagishi, K. Watanabe, T. Taniguchi, P. Jarillo-Herrero, P. Jacquod, B.J. LeRoy, *Nat. Phys.* **8**, 382 (2012)
37. B. Hunt, J.D. Sanchez-Yamagishi, A.F. Young, M. Yankowitz, B.J. LeRoy, K. Watanabe, T. Taniguchi, P. Moon, M. Koshino, P. Jarillo-Herrero, R.C. Ashoori, *Science* **340**(80), 1427 (2013)
38. L.A. Ponomarenko, R.V. Gorbachev, G.L. Yu, D.C. Elias, R. Jalil, A.A. Patel, A. Mishchenko, A.S. Mayorov, C.R. Woods, J.R. Wallbank, M. Mucha-Kruczynski, B.A. Piot, M. Potemski, I.V. Grigorieva, K.S. Novoselov, F. Guinea, V.I. Fal'ko, A.K. Geim, *Nature* **497**, 594 (2013)
39. K. Kim, M. Yankowitz, B. Fallahazad, S. Kang, H.C.P. Movva, S. Huang, S. Larentis, C.M. Corbet, T. Taniguchi, K. Watanabe, S.K. Banerjee, B.J. LeRoy, E. Tutuc, *Nano Lett.* **16**, 1989 (2016)
40. D. Wang, G. Chen, C. Li, M. Cheng, W. Yang, S. Wu, G. Xie, J. Zhang, J. Zhao, X. Lu, P. Chen, G. Wang, J. Meng, J. Tang, R. Yang, C. He, D. Liu, D. Shi, K. Watanabe, T. Taniguchi, J. Feng, Y. Zhang, G. Zhang, *Phys. Rev. Lett.* **116**, 126101 (2016)
41. C.R. Woods, F. Withers, M.J. Zhu, Y. Cao, G. Yu, A. Kozikov, M. Ben Shalom, S.V. Morozov, M.M. van Wijk, A. Fasolino, M.I. Katsnelson, K. Watanabe, T. Taniguchi, A.K. Geim, A. Mishchenko, K.S. Novoselov, *Nat. Commun.* **7**, 10800 (2016)
42. E.Y. Andrei, D.K. Efetov, P. Jarillo-Herrero, A.H. MacDonald, K.F. Mak, T. Senthil, E. Tutuc, A. Yazdani, A.F. Young, *Nat. Rev. Mater.* **6**, 201 (2021)
43. Z. Liu, F. Liu, and Y. S. Wu, *Chinese Phys. B* (2014).
44. S. Deng, A. Simon, and J. Köhler, *J. Solid State Chem.* (2003).
45. M. Kang, S. Fang, L. Ye, H. C. Po, J. Denlinger, C. Jozwiak, A. Bostwick, E. Rotenberg, E. Kaxiras, J. G. Checkelsky, and R. Comin, *Nat. Commun.* (2020).
46. S. Miyahara, S. Kusuta, and N. Furukawa, *Phys. C Supercond. Its Appl.* (2007).
47. S. Zhang, H. H. Hung, and C. Wu, *Phys. Rev. A - At. Mol. Opt. Phys.* (2010).
48. W. Wang, B. Wang, Z. Gao, G. Tang, W. Lei, X. Zheng, H. Li, X. Ming, and C. Autieri, *Phys. Rev. B* (2020).
49. W. H. Han, S. Kim, I. H. Lee, and K. J. Chang, *ArXiv* (2019).
50. Y. Cao, V. Fatemi, S. Fang, K. Watanabe, T. Taniguchi, E. Kaxiras, and P. Jarillo-Herrero, *Nature* (2018).
51. Y. Choi, J. Kemmer, Y. Peng, A. Thomson, H. Arora, R. Polski, Y. Zhang, H. Ren, J. Alicea, G. Refael, F. von Oppen, K. Watanabe, T. Taniguchi, and S. Nadj-Perge, *Nat. Phys.* (2019).
52. Y. Cao, J. Y. Luo, V. Fatemi, S. Fang, J. D. Sanchez-Yamagishi, K. Watanabe, T. Taniguchi, E. Kaxiras, and P. Jarillo-Herrero, *Phys. Rev. Lett.* (2016).
53. E. Laksono, J. N. Leaw, A. Reaves, M. Singh, X. Wang, S. Adam, and X. Gu, *Solid State Commun.* (2018).
54. M. H. Naik and M. Jain, *Phys. Rev. Lett.* (2018).
55. A. Splendiani, L. Sun, Y. Zhang, T. Li, J. Kim, C.Y. Chim, G. Galli, F. Wang, *Nano Lett.* **10**, 1271 (2010)
56. H.R. Gutierrez, N. Perea-Lopez, A.L. Elias, A. Berkdemir, B. Wang, R. Lv, F. Lopez-Urias, V.H. Crespi, H. Terrones, M. Terrones, *Nano Lett.* **13**, 3447 (2012)
57. R. Debbarma, S.K. Behura, Y. Wen, S. Che, V. Berry, *Nanoscale* **10**, 20218 (2018)
58. S. Behura, K.C. Chang, Y. Wen, R. Debbarma, P. Nguyen, S. Che, S. Deng, M.R. Seacrist, V. Berry, I.E.E.E. *Nanotechnol. Mag.* **11**, 33 (2017)
59. L. Yuan, B. Zheng, J. Kunstmann, T. Brumme, A. B. Kuc, C. Ma, S. Deng, D. Blach, A. Pan, and L. Huang, *Nat. Mater.* (2020).
60. J. Choi, M. Florian, A. Steinhoff, D. Erben, K. Tran, L. Sun, J. Quan, R. Claassen, S. Majumder, J. A. Hollingsworth, T. Taniguchi, K. Watanabe, K. Ueno, A. Singh, G. Moody, F. Jahnke, and X. Li, *ArXiv* (2020).
61. K. Tran, J. Choi, and A. Singh, *ArXiv* (2020).
62. F. Wu, T. Lovorn, and A. H. MacDonald, *Phys. Rev. Lett.* (2017).
63. A. Tartakovskii, *Nat. Rev. Phys.* (2020).
64. K. Tran, G. Moody, F. Wu, X. Lu, J. Choi, K. Kim, A. Rai, D.A. Sanchez, J. Quan, A. Singh, J. Embley, A. Zepeda, M. Campbell, T. Autry, T. Taniguchi, K. Watanabe, N. Lu, S.K. Banerjee, K.L. Silverman, S. Kim, E. Tutuc, L. Yang, A.H. MacDonald, X. Li, *Nature* **567**, 71 (2019)
65. K.L. Seyler, P. Rivera, H. Yu, N.P. Wilson, E.L. Ray, D.G. Mandrus, J. Yan, W. Yao, X. Xu, *Nature* **567**, 66 (2019)
66. Xu, X.; Yao, W.; Xiao, D.; Heinz, T. F. Spin and Pseudospins in Layered Transition Metal Dichalcogenides. *Nature Physics*, **10**, 343–350 (2014). <https://doi.org/10.1038/nphys2942>
67. E.M. Alexeev, D.A. Ruiz-Tijerina, M. Danovich, M.J. Hamer, D.J. Terry, P.K. Nayak, S. Ahn, S. Pak, J. Lee, J.I. Sohn, M.R. Molas, M. Koperski, K. Watanabe, T. Taniguchi, K.S. Novoselov, R.V. Gorbachev, H.S. Shin, V.I. Fal'ko, A.I. Tartakovskii, *Nature* **567**, 81 (2019)
68. Ni, G. X.; McLeod, A. S.; Sun, Z.; Wang, L.; Xiong, L.; Post, K. W.; Sunku, S. S.; Jiang, B. Y.; Hone, J.; Dean, C. R.; Fogler, M. M.; Basov, D. N. Fundamental Limits to Graphene Plasmonics. *Nature*, **557**, 530–533 (2018). <https://doi.org/10.1038/s41586-018-0136-9>
69. Dai, S.; Fang, W.; Rivera, N.; Stehle, Y.; Jiang, B. Y.; Shen, J.; Tay, R. Y.; Ciccarino, C. J.; Ma, Q.; Rodan-Legrain, D.; Jarillo-Herrero, P.; Teo, E. H. T.; Fogler, M. M.; Narang, P.; Kong, J.; Basov, D. N. Phonon Polaritons in Monolayers of Hexagonal Boron Nitride. *Adv. Mater.*, **31**(37) (2019). <https://doi.org/10.1002/adma.201806603>
70. Li, P.; Lewin, M.; Kretinin, A. V.; Caldwell, J. D.; Novoselov, K. S.; Taniguchi, T.; Watanabe, K.; Gaussmann, F.; Taubner, T. Hyperbolic Phonon-Polaritons in Boron Nitride for near-Field Optical Imaging and Focusing. *Nature Communications*, **6**, Article number: 7507 (2015). <https://doi.org/10.1038/ncomms8507>
71. Dai, S.; Fei, Z.; Ma, Q.; Rodin, A. S.; Wagner, M.; McLeod, A. S.; Liu, M. K.; Gannett, W.; Regan, W.; Watanabe, K.; Taniguchi, T.; Thieme, M.; Dominguez, G.; Castro Neto, A. H.; Zettl, A.; Keilmann, F.; Jarillo-Herrero, P.; Fogler, M. M.; Basov, D. N. Tunable Phonon Polaritons in Atomically Thin van Der Waals Crystals of Boron Nitride. *Science*, **343**, (6175), 1125–1129 (2014). <https://doi.org/10.1126/science.1246833>
72. Giles, A. J.; Dai, S.; Vurgaftman, I.; Hoffman, T.; Liu, S.; Lindsay, L.; Ellis, C. T.; Assefa, N.; Chatzakakis, I.; Reinecke, T. L.; Tischler, J. G.; Fogler, M. M.; Edgar, J. H.; Basov, D. N.; Caldwell, J. D. Ultralow-Loss Polaritons in Isotopically Pure Boron Nitride. *Nature Materials*, **17**, 134–139 (2018). <https://doi.org/10.1038/NMAT5047>
73. Jia, Y.; Zhao, H.; Guo, Q.; Wang, X.; Wang, H.; Xia, F. Tunable Plasmon-Phonon Polaritons in Layered Graphene-Hexagonal Boron Nitride Heterostructures. *ACS Photonics*, **2**(7), 907–912 (2015). <https://doi.org/10.1021/acsp Photonics.5b00099>
74. Dufferwiel, S.; Lyons, T. P.; Solnyshkov, D. D.; Trichet, A. A. P.; Withers, F.; Schwarz, S.; Malpuech, G.; Smith, J. M.; Novoselov, K. S.; Skolnick, M. S.; Krizhanovskii, D. N.; Tartakovskii, A. I. Valley-Addressable Polaritons in Atomically Thin Semiconductors. *Nature Photonics*, **11**, 497–501 (2017). <https://doi.org/10.1038/nphoton.2017.125>

75. Gartstein, Y. N.; Li, X.; Zhang, C. Exciton Polaritons in Transition-Metal Dichalcogenides and Their Direct Excitation via Energy Transfer. *Phys. Rev. B*, **92**, 075445 (2015). <https://doi.org/10.1103/PhysRevB.92.075445>
76. Dufferwiel, S.; Lyons, T. P.; Solnyshkov, D. D.; Trichet, A. A. P.; Catanzaro, A.; Withers, F.; Malpuech, G.; Smith, J. M.; Novoselov, K. S.; Skolnick, M. S.; Krizhanovskii, D. N.; Tartakovskii, A. I. Valley Coherent Exciton-Polaritons in a Monolayer Semiconductor. *Nature Communications*, **9**, Article number: 4797 (2018). <https://doi.org/10.1038/s41467-018-07249-z>
77. Hu, F.; Fei, Z. Recent Progress on Exciton Polaritons in Layered Transition-Metal Dichalcogenides. *Advanced Optical Materials*, **8**(5) (2020). <https://doi.org/10.1002/adom.201901003>
78. Epstein, I.; Chaves, A. J.; Rhodes, D. A.; Frank, B.; Watanabe, K.; Taniguchi, T.; Giessen, H.; Hone, J. C.; Peres, N. M. R.; Koppens, F. H. L. Highly Confined In-Plane Propagating Exciton-Polaritons on Monolayer Semiconductors. *2D Materials*, **7**(3), 035031 (2020). <https://doi.org/10.1088/2053-1583/ab8dd4>
79. Sunku, S. S.; Ni, G. X.; Jiang, B. Y.; Yoo, H.; Sternbach, A.; McLeod, A. S.; Stauber, T.; Xiong, L.; Taniguchi, T.; Watanabe, K.; Kim, P.; Fogler, M. M.; Basov, D. N. Photonic Crystals for Nano-Light in Moiré Graphene Superlattices. *Science*, **362**(6419), 1153–1156 (2018). <https://doi.org/10.1126/science.aau5144>
80. Hu, F.; Das, S. R.; Luan, Y.; Chung, T. F.; Chen, Y. P.; Fei, Z. Real-Space Imaging of the Tailored Plasmons in Twisted Bilayer Graphene. *Phys. Rev. Lett.*, **119**, 247402 (2017). <https://doi.org/10.1103/PhysRevLett.119.247402>
81. Huang, B.; Clark, G.; Klein, D. R.; MacNeill, D.; Navarro-Moratalla, E.; Seyler, K. L.; Wilson, N.; McGuire, M. A.; Cobden, D. H.; Xiao, D.; Yao, W.; Jarillo-Herrero, P.; Xu, X. Electrical Control of 2D Magnetism in Bilayer CrI<sub>3</sub>. *Nature Nanotechnology*, **13**, 544–548 (2018). <https://doi.org/10.1038/s41565-018-0121-3>
82. Wang, Z.; Gutiérrez-Lezama, I.; Ubrig, N.; Kroner, M.; Gibertini, M.; Taniguchi, T.; Watanabe, K.; Imamoğlu, A.; Giannini, E.; Morpurgo, A. F. Very Large Tunneling Magnetoresistance in Layered Magnetic Semiconductor CrI<sub>3</sub>. *Nature Communications*, **9**, Article number: 2516 (2018). <https://doi.org/10.1038/s41467-018-04953-8>
83. McGuire, M. A.; Dixit, H.; Cooper, V. R.; Sales, B. C. Coupling of Crystal Structure and Magnetism in the Layered, Ferromagnetic Insulator CrI<sub>3</sub>. *Chem. Mater.*, **27**(2), 612–620 (2015). <https://doi.org/10.1021/cm504242t>
84. Ghazaryan, D.; Greenaway, M. T.; Wang, Z.; Guarochico-Moreira, V. H.; Vera-Marun, I. J.; Yin, J.; Liao, Y.; Morozov, S. V.; Kristanovski, O.; Lichtenstein, A. I.; Katsnelson, M. I.; Withers, F.; Mishchenko, A.; Eaves, L.; Geim, A. K.; Novoselov, K. S.; Misra, A. Magnon-Assisted Tunnelling in van Der Waals Heterostructures Based on CrBr<sub>3</sub>. *Nature Electronics*, **1**, 344–349 (2018). <https://doi.org/10.1038/s41928-018-0087-z>
85. K. Sreenivas, *Bull. Mater. Sci.* **15**, 287 (1992)
86. S. Oh, H. Hwang, I.K. Yoo, *APL Mater.* **7**, 91109 (2019)
87. K.T. Butler, J.M. Frost, A. Walsh, *Energy Environ. Sci.* **8**, 838 (2015)
88. M. Osada, T. Sasaki, *APL Mater.* **7**, 120902 (2019)
89. Z. Guan, H. Hu, X. Shen, P. Xiang, N. Zhong, J. Chu, C. Duan, *Adv. Electron. Mater.* **6**, 1900818 (2020)
90. C. Cui, F. Xue, W.-J. Hu, L.-J. Li, *Npj 2D Mater. Appl.* **2**, 18 (2018)
91. Z. Zheng, Q. Ma, Z. Bi, S. de la Barrera, M.-H. Liu, N. Mao, Y. Zhang, N. Kiper, K. Watanabe, T. Taniguchi, J. Kong, W.A. Tisdale, R. Ashoori, N. Gedik, L. Fu, S.-Y. Xu, P. Jarillo-Herrero, *Nature* **588**, 71 (2020)
92. Yasuda, K.; Wang, X.; Watanabe, K.; Taniguchi, T.; Jarillo-Herrero, P. Stacking-Engineered Ferroelectricity in Bilayer Boron Nitride. *Science*, **372**(6549), 1458–1462 (2021). <https://doi.org/10.1126/science.abd3230>
93. Editorial: 2D Magnetism Gets Hot. *Nature Nanotechnology*, **13**, 269 (2018). <https://doi.org/10.1038/s41565-018-0128-9>
94. M. Gibertini, M. Koperski, A.F. Morpurgo, K.S. Novoselov, *Nat. Nanotechnol.* **14**, 408 (2019)
95. K.F. Mak, J. Shan, D.C. Ralph, *Nat. Rev. Phys.* **1**, 646 (2019)
96. M. Galbiati, V. Zlatko, F. Godel, P. Hirschauer, A. Vecchiola, K. Bouzehouane, S. Collin, B. Servet, A. Cantarero, F. Petroff, M.-B. Martin, B. Dlubak, P. Seneor, A.C.S. Appl. Electron. Mater. **2**, 3508 (2020)
97. J. Su, M. Wang, G. Liu, H. Li, J. Han, T. Zhai, *Adv. Sci.* **7**, 2001722 (2020)
98. A. Nimbalkar, H. Kim, *Nano-Micro Lett.* **12**, 126 (2020)
99. D.S. Schulman, A.J. Arnold, S. Das, *Chem. Soc. Rev.* **47**, 3037 (2018)
100. A. Allain, J. Kang, K. Banerjee, A. Kis, *Nat. Mater.* **14**, 1195 (2015)